Supporting Information

Lu et al. 10.1073/pnas.0908848106

SI Text

Materials and Methods

Radioactive Labeling of Seeds. Seeds were harvested into ice-cold 50 mM MES buffer (pH 5.0) and then transferred to fresh buffer containing either 0.02 mM [1-^{14}C]glycerol and 0.5 mM acetate or 0.5 mM [1-^{14}C]acetate and 0.02 mM glycerol at 25 °C. After a 15-min pulse labeling, the seeds were transferred to unlabelled media for the chase. Samples were harvested in liquid nitrogen at varying time intervals. Total lipids were extracted and separated by silica-TLC using a solvent system of acetone:water (100:4 by volume) for neutral lipids or chloroform:methanol:water (50:50:10 by volume) for polar lipids. After the plates were scraped, PC, DAG, and TAG radioactivity was determined by scintillation counting.

Mapping of the *rod1* Locus. Initial screening by bulk segregant analysis of a set of 20 simple sequence length polymorphism (SSLP) markers that are evenly distributed in the *Arabidopsis* genome resulted in the linkage of *rod1* to the marker NGA162 on chromosome 3. To fine-map the *rod1* locus, we identified 196 individual F2 plants that were homozygous at the *rod1* locus, as indicated by increased 18:1 in seed fatty acid composition. Segregation analysis using available polymorphic SSLP markers in the vicinity of NGA162 delimited the *rod1* mutation to an interval between NGA162 and NT204. We then designed more polymorphic markers using PCR primers, and subsequently located the *rod1* locus in the region of chromosome 3 covered by BAC clones MJK13, MQD17, and MSJ11. This allowed us to identify the ROD1 locus through a candidate gene approach. To confirm At3g15820 as the *ROD1* locus, a 3,961-bp PCR fragment containing the At3g15820 gene was amplified using genomic DNA extracted from Col-0 WT plants. This genomic fragment was cloned into a binary vector, pGate-Phas-DsRed (1), at the AflII and *Eco*RI sites and then transferred into *Agrobacterium tumefaciens* strain GV3101 (pMP90) for transformation of *rod1* mutant plants. Transformants were selected based on DsRed expression (2). Fatty acyl methyl esters derived from individual seeds of 10 red transgenic seeds and 3 brown nontransgenic seeds were used to determine seed fatty acid composition using gas chromatography.

Enzyme Activity Assays for ROD1 Protein. To test whether ROD1 has PAP activity, the cDNA of At3g15820 was cloned by RT-PCR using mRNA extracted from WT developing seeds. Then the PCR fragment was ligated into the HindIII/XhoI sites of the pYES2 vector (Invitrogen) for expression in yeast under the *GAL1* promoter. The resulting construct and pYES2 vector were transformed into the *dpp1*Δ *lpp1*Δ double-mutant strain (kindly provided by Dr. G. Carmen, Rutgers University) using the *S.c.* EasyComp Transformation Kit (Invitrogen). This strain has reduced PAP activity and is suitable for assaying the activity of the *Arabidopsis* PAP (AtLPP1) (3). Yeast cultures were grown at 28 °C in complete Synthetic Defined medium (uracil-tryptophan-histidine) supplemented with 2% glucose. Total membrane fraction was obtained from exponential-phase yeast cells after galactose induction for 6 h, as described previously (4). PAP activity assays were carried out as described previously (5). The results, shown in Fig. S1, indicate that ROD1 does not have PAP activity. At3g15830 also does not have PAP activity under the same assay conditions.

For CPT and PDCT assays, yeast cells were inoculated from overnight cultures and grown to mid-log phase (OD_{600} = 0.5–1.5) by rotary shaking at 30 °C in liquid synthetic minimal media lacking uracil and tryptophan and supplemented with 2% glucose (Clontech). To prepare microsomes, yeast cells were harvested by centrifugation for 10 min at 1,000 × *g*. The cell pellet was washed once with sterile water and then resuspended in ice-cold glucose-Tris-EDTA (GTE) buffer [20% glycerol, 50 mM Tris-HC1 (pH 7.4), 1 mM EDTA] to prepare the membrane fraction using glass beads. CDP-CPT assays were conducted using 0.1 μmol diolein and 1 nmol [^{14}C]CDP-choline as substrates.

The PDCT activities in membrane preparations of HJ091 cells transformed with p424GPD (control) or p424ROD1 were determined as the amount of [^{14}C]dioleoyl-PC produced from [^{14}C-glycerol]diolein (reaction A) or [^{14}C-choline]dimyristoylphosphatidylcholine (reaction B). The substrates of 1.8 nmol (200,000 cpm) [^{14}C-glycerol]diolein (American Radiolabeled Chemicals) and 0.1 μmol dioleoyl-PC (reaction A) or 0.1 μmol diolein and 1 nmol [^{14}C-choline]di-14:0-PC and 0.1 μmol dioleoyl-PC (reaction B) were dried under nitrogen gas and resuspended in 50 μL of 4× reaction buffer [final concentrations: 50 mM 3-(*N*-morpholino)propanesulfonic acid (MOPS)/NaOH (pH 7.5), 20 mM $MgCl_2$, 0.45% Triton X-100] with the aid of a sonicating bath (6). Reactions (200 μL) were started by adding 20–250 μg of microsomal proteins suspended in the GTE buffer. Unless indicated otherwise (Fig. S1), assays were incubated at 15 °C for 15 min and were terminated by the addition of 3 mL of chloroform/ethanol (2:1, vol./vol.), followed by 1.5 mL of 0.9% KCl. Tubes were mixed by vortexing, and phase separation was facilitated by centrifugation at 2,000 × *g* for 2 min. The aqueous phase was aspirated, and the organic phase was washed twice with 1.5 mL of 40% (vol./vol.) ethanol. Samples were analyzed by TLC on silica gel plates in a solvent system of chloroform/methanol/water (65:25:4, by volume), followed by phosphorimaging analysis or radioautography. Corresponding bands were scraped, and radioactivity was determined by scintillation counting.

The effect of pH on PDCT activity was determined by using 50 mM of the following buffers: acetic acid (pH 5.0 and 5.5), MES (pH 6.0), and MOPS (pH 6.5, 7.0, 7.5, and 8.0). The reactions were carried out at 23 °C to determine the effects of pH, incubation time, and amount of microsomal proteins (Fig. S2).

Expression of *ROD1* and At3g15830. Expression data for *ROD1* (Affymetrix array element 258249_s_at) from the AtGenExpress database (accessed via Genevestigator; https://www.genevestigator.ethz.ch/) is shown in Fig. S3. The same array element also detects transcript of a second gene, At3g15830, but data from the *Arabidopsis* MPSS database (http://mpss.udel.edu/at/) indicates that this second gene is expressed only in floral tissues (data not shown). To confirm these data, we prepared RNA from germinating seedlings, rosette leaves, flowers, and green siliques of WT plants, as well as green siliques of *rod1* mutant plants. Using oligonucleotide primers specific for *ROD1* and At3g15830, we performed RT-PCR on each RNA sample using the SuperScript III one-step system (Invitrogen), according to the manufacturer's instructions. The results, shown in Fig. S4, indicate that expression of At3g15830 is restricted to the flowers, and that the transcript of this gene could not be detected in developing siliques of either WT or *rod1* plants. To test whether At3g15830 also has PDCT activity, a cDNA was cloned into the p424GPD

vector, as described above. The resulting construct, p424-At3g15830, was then transformed into HJ091, and its expression was confirmed by RT-PCR (Fig. S4, lane 16). PDCT assays using the same reaction conditions for ROD1 yielded no radiolabeled PC, indicating that the At3g15830 protein has no PDCT activity (data not shown).

Phylogenetic Analyses of ROD1-Related Proteins. Sequences were obtained from the sources indicated in Fig. S5. The methods for producing the Bayesian consensus tree (7) included using prior settings for the most complex WAG + F + I + G amino acid substitution model and letting 2 Markov chains each run for 1,000,000 generations (sufficient for the 2 separate runs to converge before the second parameter samples were made), while sampling every 10,000 generations at likelihood stationarity to avoid autocorrelated parameter estimates.

1. Lu C, Fulda M, Wallis JG, Browse J (2006) A high-throughput screen for genes from castor that boost hydroxy fatty acid accumulation in seed oils of transgenic *Arabidopsis*. *Plant J* 45:847–856.
2. Hjelmstad R, Bell R (1991) sn-1,2-diacylglycerol choline- and ethanolaminephosphotransferases in *Saccharomyces cerevisiae*: Mixed micellar analysis of the CPT1 and EPT1 gene products. *J Biol Chem* 266:4357–4365.
3. Pierrugues O, et al. (2001) Lipid phosphate phosphatases in *Arabidopsis*: Regulation of the *AtLPP1* gene in response to stress. *J Biol Chem* 276:20300–20308.
4. Toke DA, et al. (1998) Isolation and characterization of the *Saccharomyces cerevisiae LPP1* gene encoding a Mg2+-independent phosphatidate phosphatase. *J Biol Chem* 273:14331–14338.
5. Han GS, Wu WI, Carman GM (2006) The *Saccharomyces cerevisiae Lipin* homolog is a Mg2+-dependent phosphatidate phosphatase enzyme. *J Biol Chem* 281:9210–9218.
6. Swofford DL (2003) *PAUP*: Phylogenetic Analysis Using Parsimony (*and Other Methods). Version* 4 (Sinauer Associates, Sunderland, MA).
7. Ronquist F, Huelsenbeck JP (2003) MRBAYES 3: Bayesian phylogenetic inference under mixed models. *Bioinformatics* 19:1572–1574.

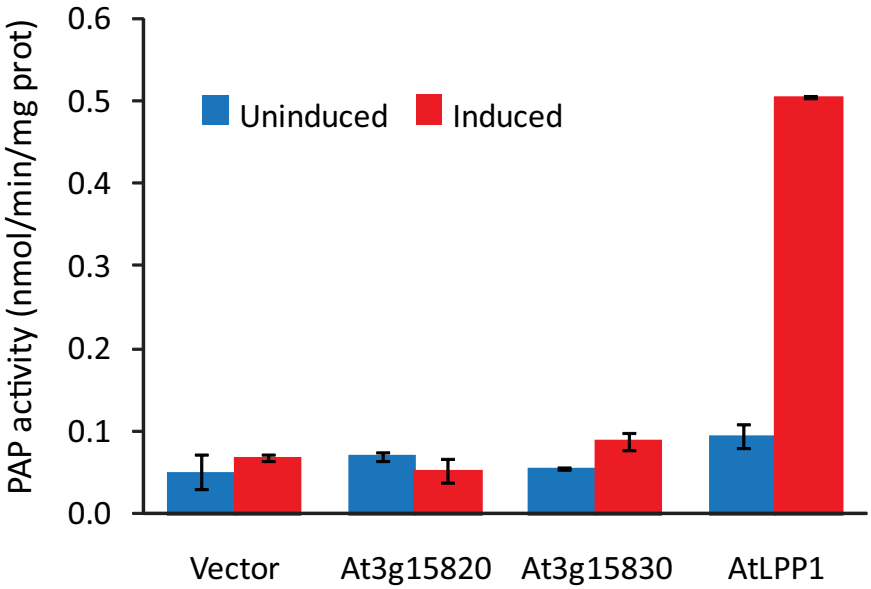

Fig. S1. PAP activity assays. PAP activity was measured in membrane fractions from yeast cells after galactose induction for 6 h. The reaction buffer contained 50 mM Tris-aleate (pH 7.0), 10 mM 2-mercaptoethanol, 0.1 mM phosphatidic acid, 1 mM TX-100, and 2 mM EDTA. Data represent mean and SD of 3 independent experiments. AtLPP1 was used as a positive control. The vector was pYES2.

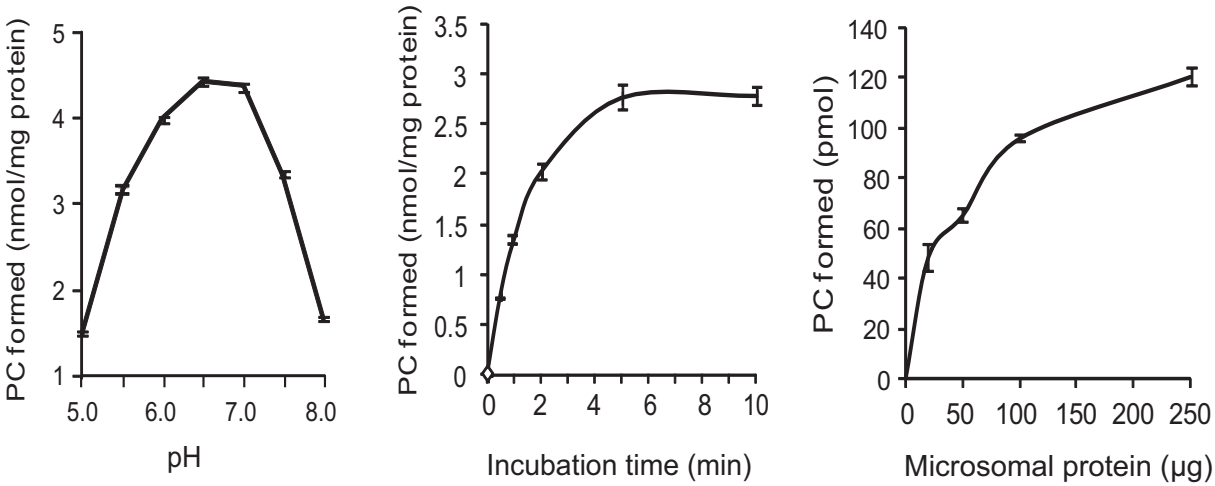

Fig. S2. Enzyme activity assays of ROD1. (*A*) The effect of pH on the PDCT activities of ROD1. (*B* and *C*) The linearity of the PDCT activity as a function of incubation time (*B*) and added microsomal protein (*C*). Data represent mean and SD of 3 independent reactions.

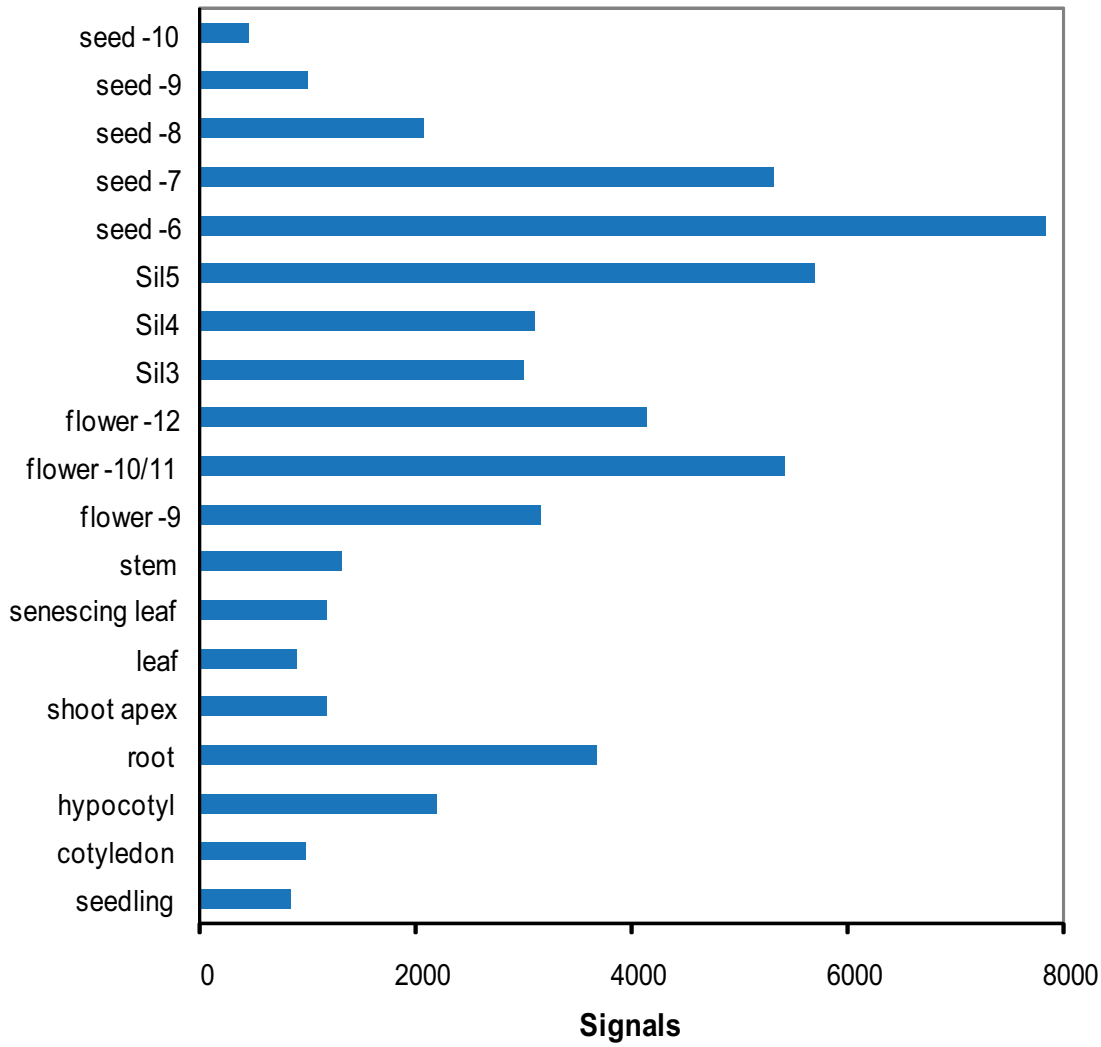

Fig. S3. Tissue-specific expression of the *ROD1* gene. Data for *ROD1* expression were obtained from AtGenExpress at the Genevestigator site (https://www.genevestigator.ethz.ch/). Signal intensities were averaged for all of the stages included in the figure.

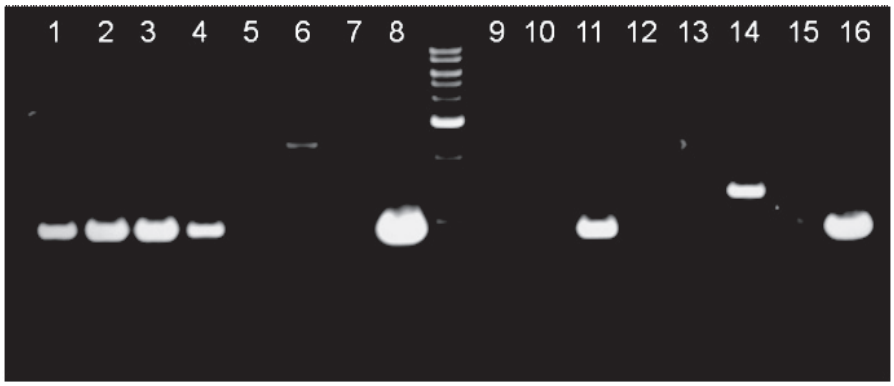

Fig. S4. RT-PCR of *ROD1* (lanes 1–8) and At3g15830 (lanes 9–16) expression in *Arabidopsis* and yeast cells. RT-PCR was performed on samples of total RNA from germinating seedlings (lanes 1 and 9), young leaves (lanes 2 and 10), flowers (lanes 3 and 11), and siliques (lanes 4 and 12) of WT *Arabidopsis*; siliques from *rod1* mutant plants (lanes 5 and 13); and yeast cells containing p424GPD (lanes 7 and 15) or p424ROD1 (lane 8) and p424-At3g15830 (lane 16). PCR using the same primers was performed on genomic DNA from *rod1* (lanes 6 and 14).

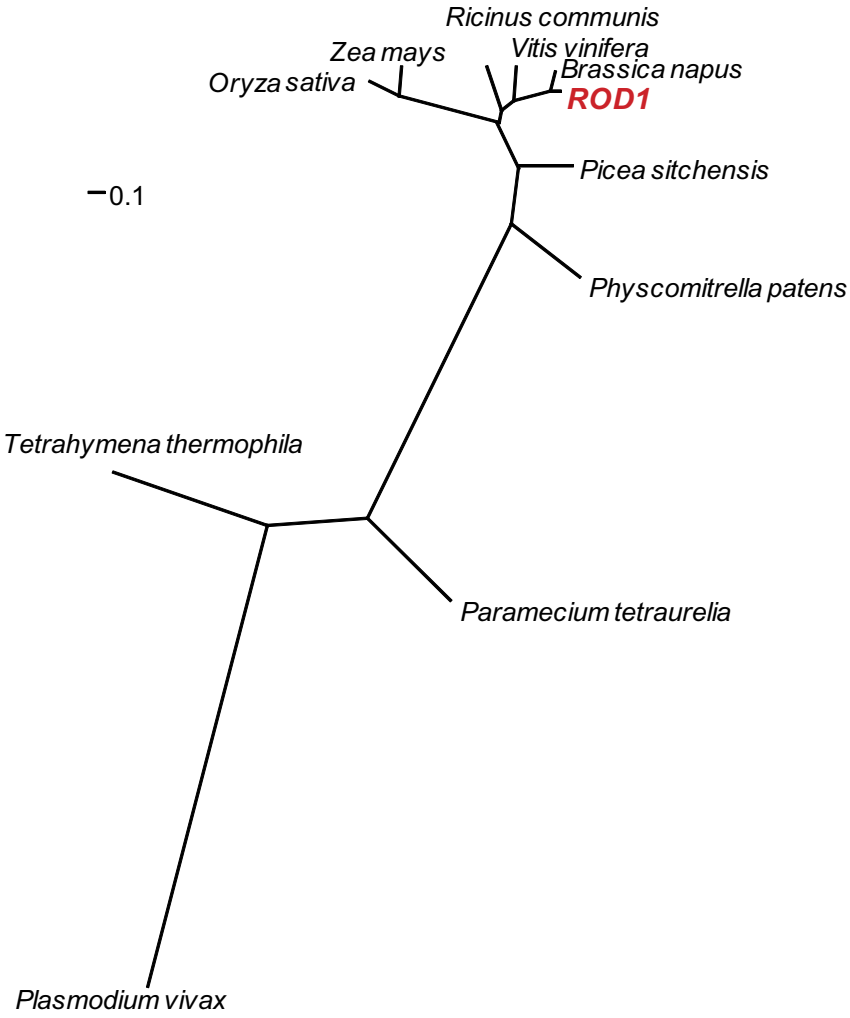

Fig. S5. Inferred phylogenetic relationship among ROD1 homologues in different organisms. The following sequences and their accession numbers are from the National Center for Biotechnology Information (http://blast.ncbi.nlm.nih.gov/Blast.cgi): *Oryza sativa* (NP_001058029), *Paramecium tetraurelia* (XP_001444992), *Physcomitrella patens* (XP_001763589), *Picea sitchensis* (ABK25679), *Plasmodium vivax* (XP_001616259), *Tetrahymena thermophila* (XP_001013603), *Vitis vinifera* (CAO62718), and *Zea mays* (ACG45691). The *Brassica napus* sequence was obtained from BrassicaDB (http://brassica.bbsrc.ac.uk/BrassicaDB/). The *Ricinus communuis* sequence was obtained from the castor bean genome database (http://castorbean.jcvi.org/).

Table S1. Fatty acid composition of leaf and root lipids is similar in *rod1* and WT

	Mol % of fatty acid species					
	16:0	16:3	18:0	18:1	18:2	18:3
Leaf						
WT	14.3 ± 0.4	13.7 ± 0.4	1.1 ± 0.1	3.8 ± 0.1	16.1 ± 0.5	46.3 ± 1.4
rod1	14.3 ± 0.3	14.8 ± 0.5	1.2 ± 0.1	3.8 ± 0.1	15.5 ± 0.4	44.9 ± 1.5
Root						
WT	22.9 ± 1.6	—	1.7 ± 0.3	7.6 ± 1.2	42.4 ± 1.5	25.7 ± 1.6
rod1	23.6 ± 0.8	—	1.3 ± 0.1	6.8 ± 0.9	39.3 ± 0.8	29.0 ± 1.0